



# Femtosecond laser stimulated anisotropy of electrolytically produced CdS polymer nanocomposites

O. M. Yanchuk<sup>1</sup> · O. V. Marchuk<sup>1</sup> · I. A. Moroz<sup>2</sup> · O. A. Vyshnevskiy<sup>3</sup> · A. M. El-Naggar<sup>4,5</sup> · A. A. Albassam<sup>4</sup> · I. V. Kityk<sup>6</sup> · P. Czaja<sup>6</sup>

Received: 5 August 2019 / Accepted: 28 August 2019 / Published online: 4 September 2019  
© The Author(s) 2019

## Abstract

Studies of two-beam coherent induced optical anisotropy has been performed for the cadmium sulphide nanocrystallites (NC) embedded within the different polymer matrices. The NC were fabricated by the modified electrolytical method and have been embedded into different polymer matrices: PC, PMMA, PVA. The phototreatment was performed by two space split coherent beams generated by 120 fs laser with pulse energy 23 nJ. The phototreatment has been durated several minutes until the clear diffraction grating has been observed. The monitoring of the laser induced gratings and of the anisotropy was performed using the cw 1150 nm continuous wave He–Ne laser with power about 30 mW. Varying the polarization of the laser coherent femtosecond beams we have found that the optimal gratings has been achieved for 45° polarizations between the beams. The control of the maximal laser induced gratings has been done using optically polarized method. The effect is not completely reversible and there remain some changes after switching off of the phototreatment. The anisotropy has been monitored by Senarmont method. The role of different polymers on the output photo stimulated birefringence was explored. This method may be promising for the design and engineering of optical triggers in the femtosecond laser pulse duration.

## 1 Introduction

The intensive development of pulsed laser operated devices [1–3] stimulates a search and design of novel optoelectronic materials for fast operated laser triggering [4]. Particular interest here present semiconducting NC embedded into the polymer matrices which form a very promising class of

polymer nanocomposites [5, 6]. It is crucial that the principal optical parameters of polymer nanocomposites include the search of both linear and nonlinear optical constants as well as the laser operated materials [7]. The main goal of such exploration consists in the design of nanocomposites with the low power switching parameters [8]. This may be effectively achieved by formation of optical anisotropy using

✉ I. V. Kityk  
ikityk@el.pcz.czest.pl; iwank74@gmail.com

O. M. Yanchuk  
yanchuk59@gmail.com

O. V. Marchuk  
Oleg\_M\_1974@i.ua

I. A. Moroz  
moroz.iryana1@gmail.com

O. A. Vyshnevskiy  
vyshnevskyy@i.ua

A. M. El-Naggar  
amelnaggar@yahoo.com; elnaggar@ksu.edu.sa

P. Czaja  
czajap@el.pcz.czest.pl

<sup>1</sup> Department of Inorganic and Physical Chemistry, Eastern European National University, 13 Voli Avenue, Lutsk 43025, Ukraine

<sup>2</sup> Department of Materials Science, Lutsk National Technical University, 75 L'vivs'ka Str., Lutsk 43018, Ukraine

<sup>3</sup> M.P. Semenenko Institute of Geochemistry, Mineralogy and Ore Formation, NAS of Ukraine, Kiev, Ukraine

<sup>4</sup> Research Chair of Exploitation of Renewable Energy Applications in Saudi Arabia, Physics & Astronomy Department, College of Science, King Saud University, P.O. Box 2455, Riyadh 11451, Saudi Arabia

<sup>5</sup> Physics Department, Faculty of Science, Ain Shams University, Abbasia, Cairo 11566, Egypt

<sup>6</sup> Faculty of Electrical Engineering, Institute of Optoelectronics and Measuring Systems, Czestochowa University of Technology, Armii Krajowej 17 Str., 42-200 Czestochowa, Poland

the two-beam color treatment at different angles [9]. Because the traditional nanosecond lasers possess relatively high parasitic photo-thermal destruction and recently very huge efforts have been devoted to the search of the femtosecond laser operated materials [10].

Due to relatively low (120 fs) pulse time duration the effects of thermo-heating are almost completely eliminated. The principal role for the laser induced applications play interfaces between the NC and surrounding polymer matrices which may be varied by different technological processes in different polymer matrices [11]. Here very crucial role begins to play a thin layer of NC on the border with different surrounding polymer matrices [12]. Normally the dipole moments of the ground as well as excited states show here a huge enhancement which determines the laser stimulated efficiencies including multi-photon processes [13]. At the same time between the polymer matrix and the NC there occurs a huge interface potential which favors the enhanced output laser stimulated abilities. For the occurrence of material anisotropy principal role begin to play bicolor coherent laser treatment at different angles because it forms an anisotropic and acentric gratings. As a consequence in this work we perform studies of the two-beam laser stimulated anisotropy by continuous wave low power beams for probing continuous wave He–Ne lasers at wavelength 1150 nm. The studies will be performed in order to achieve maximal possible optical anisotropy.

The possible ways for enhancement of the laser stimulated birefringence will be discussed and their relaxation features after the switching off of the femtosecond laser induction are also studied. The changes of the NC aggregates were explored also by TEM before and after illumination.

### 1.1 Sample preparation

The studied CdS NC specimens have been prepared from aqueous sodium chloride (58.442 g/L or 1.0 mol/L) and thiourea (15.22 g/L or 0.20 M) with a soluble cadmium anode and ATLAS G3300 (1.0 g/L) as a likely stabilizer of particle growth at 363.2 K at current density of 0.19 A/cm<sup>2</sup> with a different time of electrolysis. Some principal synthesis parameters are presented in Table 1.

Sodium chloride, thiourea and ATLAS G3300 were transferred to a 1 L volumetric flask and dissolved in hot distilled

water. The contents of the flask were brought to the mark at the experimental temperature (90 °C) in a thermostat.

The prepared solution was transferred to the electrolyzer, which is a glass with a capacity of 400 mL. Two cylindrical electrodes, one cadmium anode, and the second, a stainless steel cathode with a surface area of 5 cm<sup>2</sup>, were immersed into the same glass. The electrodes were mounted in a cover having openings for a contact thermometer. To power the electrolyzer we have used a DC source B5-46.

The electrolyser with the immersed electrodes and a thermometer were placed into a thermostat for thermo stabilization. After heating to a desired temperature, the timer and the power source were switched on at fixed current and voltage. Upon anode dissolution orange particles immediately began to grow around it. When the synthesis time had been reached a saturation, the electrolyzer was removed from the thermostat and left to cool up to ambient temperature.

After cooling, the contents of the glass, in which the electrolysis took place, was poured into a larger glass with distilled water and left until the next day to completely settle the powder. The next day the powder was settled on the bottom of the glass and the solution over the powder poured and has been poured into a glass of distilled water. The resulting suspension was left to defend until the next day. The washing of the powdered precipitate was carried out as long as the solution, which was poured from the glass, stopped foaming. Afterwards the precipitate was transferred to a Petri dish and dried at 50 °C. The cadmium electrode was washed with distilled water, dried in air and weighed [14].

Synthesized orange powders were explored by scanning electron microscopy (SEM) and X-ray powder diffraction (diffractometer DRON-4-13, Cu-K<sub>α</sub> radiation). The morphology and sizes of synthetic CdS were also determined. Before the imaging samples were coated, using sputtering method, by platinum film of 30 Å thickness. Operating conditions of imaging were as follows: SE mode, 10 kV accelerating voltage and a 0.65 nA beam current.

The such obtained powders have been embedded into three different polymers—polymethylmethacrylate (PMMA), polyvinyl alcohol (PVA) and polycarbonate (PC). The powders have been incorporated into the corresponding polymers with photo initiators in liquid phase polymer matrix and applying the spin coating method as described in the ref. [15]. After they have been solidified by UV light with power about 45 W during the 5 min. The control of their sizes before and after the phototreatment had been done by a TEM method similar to the described in the ref. [16]. The control of their sizes before and after the phototreatment had been done by a TEM method and effect has been demonstrated maximal changes for 45% of NC by TEM 2000EX with an accelerating voltage of 100–1600 kV. The effect has shown maximal changes for 45% of NC.

**Table 1** Basic conditions of the electrochemical synthesis for the studied cadmium sulphide NC

ATLAS (g/L)	1.0			
Sample N	M6	M8	M10	M12
τ (min)	30	40	50	60
Voltage U (V)	3.8	3.5	3.4	3.4

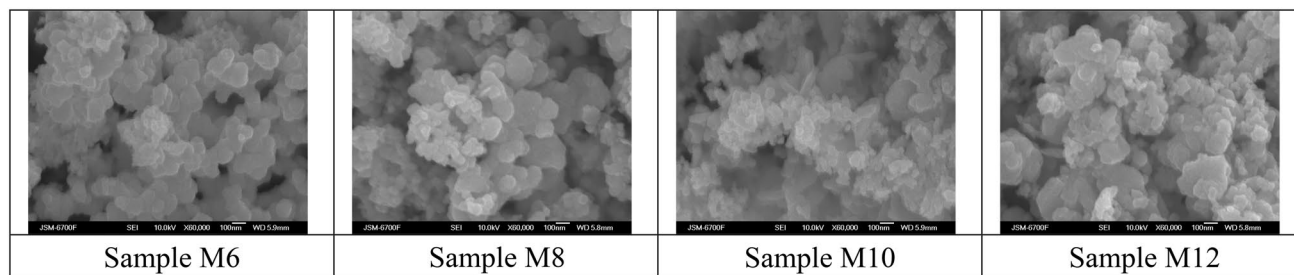


**Fig. 1** SEM images samples of CdS NC synthesized under the same ATLAS content (1.0 g/L), temperature (90 °C), current density (0.19 A/cm<sup>2</sup>), concentration NaCl (1.0 M) and thiourea (0.2 M) but differ-

ent electrolysis time (min): sample M06–30, sample M08–40, sample M10–50 and M12–60

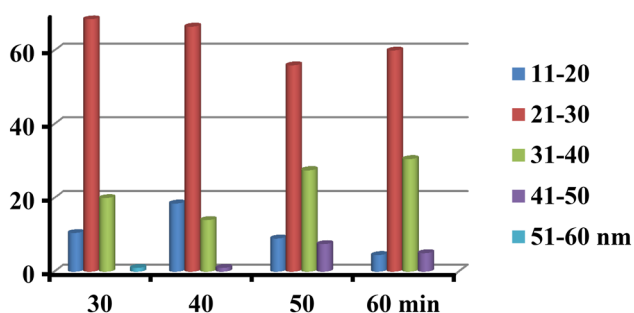


**Fig. 2** The distribution of the number of CdS NC (as a percentage of the total number of particles) in the five ranges from 11 to 60 nm

## 2 Results and discussion

### 2.1 Sample characterization

The NC powder particles possessed sizes varying in a wide range—5–60 nm. As shown in Fig. 1 particles are predominantly of flake-like form. The average diameter of the flakes was varied within 11/60 nm and the thickness—within 2/20 nm. An increase of electrolysis time has a little effect only on the sizes and their dispersion of the synthesized particles and their aggregation.

The distribution of the number of particles (as a percentage of the total number of particles) in the five different ranges from 11 to 60 nm with increment 10 nm indicates that the largest number of particles exists in the range from 21 to 30 nm (Fig. 2). The average diameter of the particles is varied in a rather narrow range—from 24 to 27 nm.

Spread of particles in size, as seen from Fig. 2, is insignificant. The Atlas 3300 is a good particle size stabilizer.

XRD diffractograms for all four samples are presented in Fig. 3. Diffraction patterns for all the samples corresponding to experimental powder pattern are indicated by blue line and correspond to the theoretical pattern

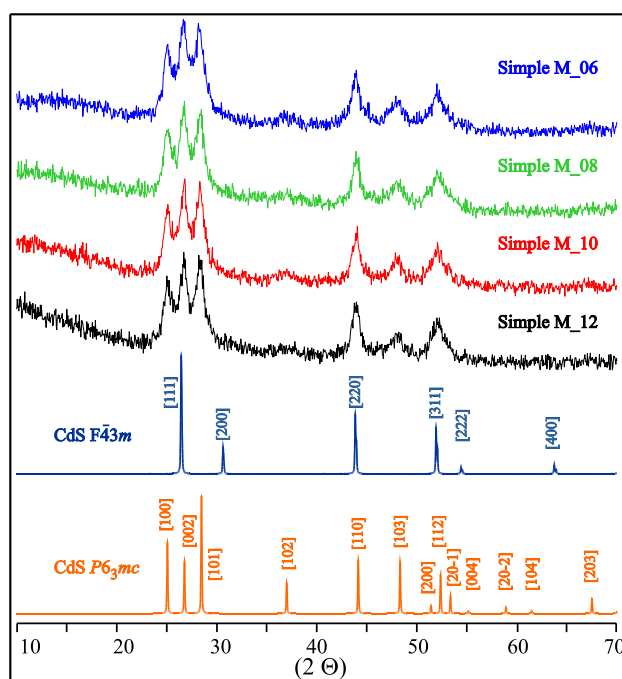


**Fig. 3** Experimental and theoretical X-ray powder sediment samples obtained by electrolysis of sodium chloride and thiourea with cadmium anode at a temperature of 90 °C, current density 0.19 A/cm<sup>2</sup> in the presence 1 g/L ATLAS G3300 and different electrolysis time (min): sample M06–30, sample M08–40, sample M10–50, sample M12–60

for the space group  $P6_3mc$  and orange line—for  $F\bar{4}3m$  of CdS. The product has two defined crystalline hexagonal and cubic structure, of wurtzite and sphalerite type, respectively.

The photo-treatment has been carried out using a set-up presented in Fig. 4.

The light of 1045 nm femtosecond laser with frequency band pass 640 MHz was split by beam splitter (BS) for two channel (Fig. 4). The first one serves as a fundamental channel with the wavelength 1045 nm and the second one (so called

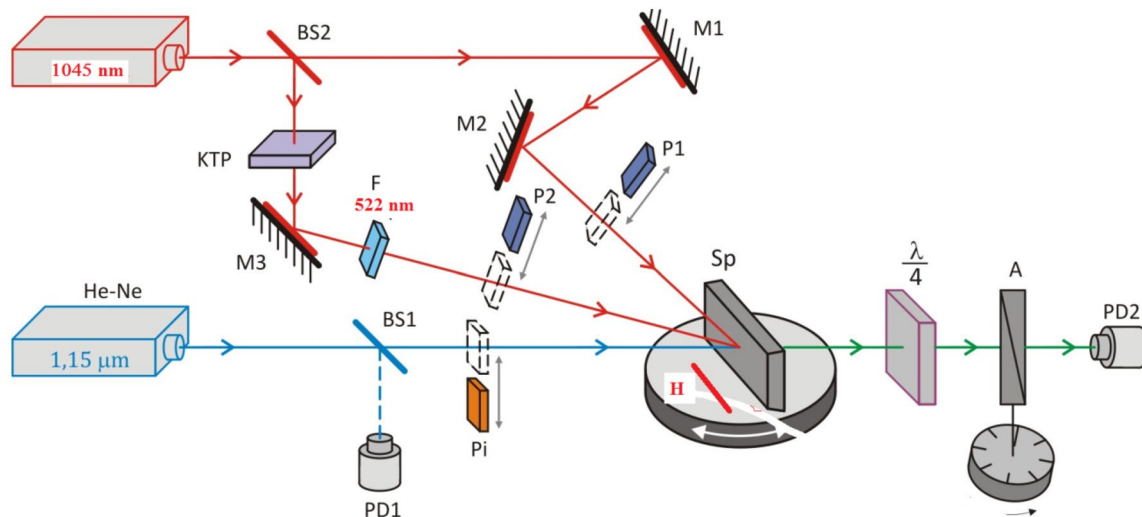


**Fig. 4** Principal set-up for the two beam femtosecond laser induced birefringence: *PD* photodiodes, 1045 nm—femtosecond laser emitting at 1045 nm, *BS* beamsplitters, *P* polarizers, *M* mirrors, *KTP* single crystals of  $\text{KTiOPO}_4$  cut under the angle of phase matching at  $\lambda = 1045$  nm

**Table 2** Principal structural parameters of titled NC

No samples	$P6_3mc$ (%)	$F\bar{4}3m$ (%)	Electrolysis time (min)
M06	71	29	30
M08	75	25	40
M10	73	27	50
M12	77	23	60

writing channel) was used for treatment by a doubled frequency coherent beam at wavelength 522 nm. The two mentioned beams were focused in the sample's surfaces within the diameter equal to about 3.5 mm which form the anisotropy due to the so called bicolor coherent optical poling

[17–19]. Additionally the TEM control of the NC allows to control the changes of sizes of the embedded NC due to photoinduced piezooptics and electrostriction.

The calculated approximate content wurtzite and sphalerite are given in Table 2.

It is clear that the structure of cadmium sulfide wurtzite prevails. The ratio of two crystalline modifications was varied from 2.4–1 to 3.3–1.

Following Fig. 5 one can see that increasing power densities of the laser stimulated beams cause significant space re-arrangement of the NC aggregates. It may be caused by laser stimulated dc-electric field due to optical poling and due to some free space of the NC embedded into the polymer matrices occurred during photosolidification. The latter was operated by time of solidification of the nanocomposites.

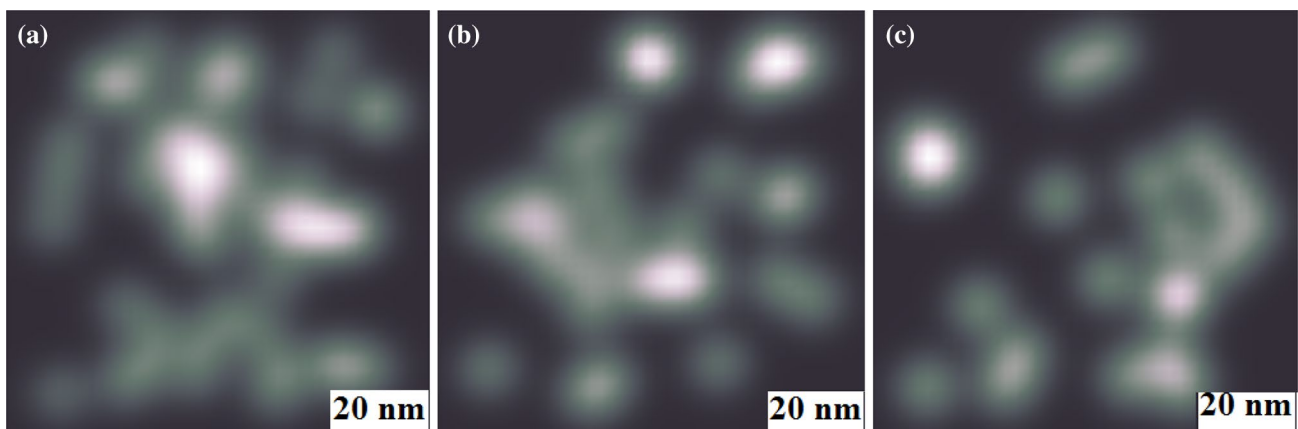


**Fig. 5** Some of the TEM images of the CdS NC at different power densities' for CdS NP polymer nanocomposites in PVA matrix: **a** before the laser treatment; **b** at power density equal to 300 MW/cm<sup>2</sup>; **c** – 500 MW/cm<sup>2</sup>

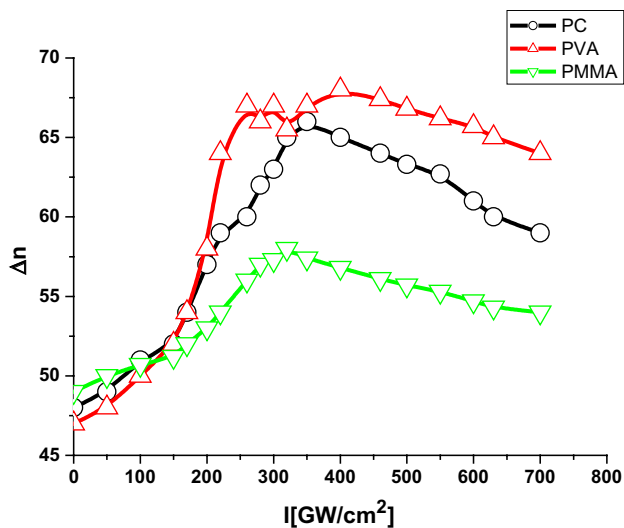


**Fig. 6** Dependence of the laser stimulated birefringence versus photoinduced laser beams for different polymer nanocomposites

After switching off of the external photoinduced beams there appears some relaxation of the NC, however it does not completely returns to initial state. This factor may be used in a future design of materials with the desired nonlinear optical features. The particular grain sizes and morphology did not influence essentially on the observed laser induced effect.

In Fig. 6 are presented the dependences of the bicolor laser stimulated birefringence versus the two beam induced power densities for the nanocomposites for different polymer matrices. At the beginning (up to 400 MW/cm<sup>2</sup>) one can see a significant increase of the birefringence and after 70 MW/cm<sup>2</sup> there occurs some saturation and even a decrease. The effect may be considered like an electrooptical effect (both linear as well as quadratic) caused by laser stimulated local dc-internal electric field strength formed by bicolor coherent beams. The electrooptical effects are very sensitive to the interface potential between the NC and the surrounding specific polymer matrix. It is clear that maximal effect exists for the PVA matrix which may be a consequence of the enhanced dipole moments determining the corresponding electrooptical coefficients. After switching off of the laser stimulated treatment there remains about 15–20% of photoinduced birefringence with respect to initial state. Here some role begins also to play photo thermal effects forming the additional space electron density acentricity favoring the increasing dipole moments. The maximal effects were observed for 45° polarization orientations between two photoinducing beams. The decrease of the laser stimulated electrooptics may be caused also by occurrence of multiphoton excitations suppressing the output optical anisotropy stimulated by electrooptics. The observed effect was at least 30% higher than observed recently for the photopolymer

olygoether acrylate composites [20] and other organic materials [21].

### 3 Conclusions

A principally novel method for formation of the optical anisotropic materials has been proposed. As a material for this goal has been used the CdS electrolytically fabricated NC embedded into the polymer PVA, PC, PMMA matrices. The phototreatment was performed by two split coherent beams generated by 120 fs laser with pulse energy 23 nJ. The phototreatment has been durated several minutes until the clear diffraction grating has been appeared. As a probing beam for optical anisotropy 1150 nm cw He–Ne laser has been used. At the beginning (up to 400 MW/cm<sup>2</sup>) one can see a significant increase of the birefringence and after 70 MW/cm<sup>2</sup> there occurs some saturation and even a decrease. The effect may be considered like an electrooptical effect (both linear as well as quadratic) caused by laser stimulated local dc-internal electric field strength bicolor beam. The electrooptical effects are very sensitive to the interface potential between the NC and the surrounding specific polymer matrix. After switching off of the laser stimulated treatment there remains about 15–20% of photoinduced birefringence with respect to initial state. Here some role begins also to play photo thermal effect forming the additional space electron density acentricity favoring the increasing dipole moments. The maximal effects were observed for 45° polarization orientations of two photoinducing beams.

**Acknowledgements** The presented results are part of a project that has received funding from the European Union’s Horizon 2020 research and innovation program under the Marie Skłodowska-Curie Grant Agreement No 778156. I.V.K. acknowledges support from resources for science in the years 2018–2022 Granted for the realization of international co-financed Project Nr W13/H2020/2018 (Dec. MNiSW 3871/H2020/2018/2). The authors are grateful to the Deanship of Scientific Research, King Saud University for funding through Vice Deanship of Scientific Research Chairs.

**Open Access** This article is distributed under the terms of the Creative Commons Attribution 4.0 International License (<http://creativecommons.org/licenses/by/4.0/>), which permits unrestricted use, distribution, and reproduction in any medium, provided you give appropriate credit to the original author(s) and the source, provide a link to the Creative Commons license, and indicate if changes were made.

### References

1. Strategies Unlimited, The Worldwide Market for Lasers: Market Review and Forecast 2016; <https://store.strategies-u.com/the-worldwide-market-for-lasers-market-review-and-forecast-2016>
2. E.Y. Zhu, Z. Tang, L. Qian, L.G. Helt, M. Liscidini, J.E. Sipe, C. Corbari, A. Canagasabay, M. Ibsen, P.G. Kazansky, Poled-fiber

- source of broadband polarization-entangled photon pairs. *Opt. Lett.* **38**, 4397–4400 (2013)
3. H. An, S. Fleming, Characterization of a second-order nonlinear layer profile in thermally poled optical fibers with second-harmonic microscopy. *Opt. Lett.* **30**, 86 (2005)
  4. S. Wang, Z. Chen, N. Chen, W. Xu, Q. Hao, S. Liu, Thermal poling of new double-hole optical fibers. *Appl. Sci.* **9**(11), 2176 (2019)
  5. M.R. Bockstaller, E.L. Thomas, Optical properties of polymer-based photonic nanocomposite materials. *J. Phys. Chem. B.* **107**, 10017–10024 (2003)
  6. Š. Meškiniš, I. Yaremchuk, V. Grigaliūnas, A. Vasiliauskas, A. Čiegis, Plasmonic properties of nanostructured diamond like carbon/silver nanocomposite films with nanohole arrays. *Mater. Sci.* **22**, 467–471 (2016)
  7. L. Xia, X. Zhang, M. Zhang, S. Dang, S. Huang, Y. Tan, W. Yan, H.L. Cui, Deep electrical modulation of terahertz wave based on hybrid metamaterial-dielectric-graphene structure. *Appl. Sci.* **9**(3), 507 (2019). <https://doi.org/10.3390/app9030507>
  8. S. Tkaczyk, M. Galceran, S. Kret, M.C. Pujol, M. Aguiló, F. Diaz, A.H. Reshak, I.V. Kityk, UV-excited piezooptical effects in oxide nanocrystals incorporated into PMMA matrices. *Acta Mater.* **56**, 5677–5684 (2008)
  9. J. Ebothe, J. Michel, I.V. Kityk, G. Lakshminarayana, O.M. Yanchuk, O.V. Marchuk, Influence of CdS nanoparticles grain morphology on laser-induced absorption. *Physica E* **100**, 69–72 (2018)
  10. D. Tan, K.N. Sharafudeen, Y. Yue, J. Qiu, Femtosecond laser induced phenomena in transparent solid materials: fundamentals and applications. *Prog. Mater. Sci.* **76**, 154–228 (2016)
  11. I.V. Kityk, Nonlinear optical phenomena in the large-sized nanocrystallites. *J. Non-Cryst. Solids* **292**, 184–201 (2001)
  12. J. Boucle, A. Kassiba, J. Emery, I.V. Kityk, M. Makowska-Janusik, J. Sanetra, N. Herlin-Boime, M. Mayne, Local electrooptic effect of the SiC large-sized nanocrystallites incorporated in polymer matrices. *Phys. Lett.* **2002**(302), 196–202 (2002)
  13. K.J. Plucinski, M. Makowska-Janusik, A. Meffeh, I.V. Kityk, V.G. Yushanin, SiON films deposited on Si(111) substrates—new promising materials for nonlinear optics. *Mater. Sci. Eng.* **1999**(VB64), 88–98 (1999)
  14. Patent 93471U Ukraine, IPC (2014.01) C 01G 11/00, Method for obtaining nanopowders of cadmium sulfide by electrolysis of an aqueous solution of indifferent electrolyte, Applicant and Patent Owner of Lesya Ukrainka Eastern European National University.—No. u201313037; Stated. 11.11.2013; Has published 10.10.2014, Byul. No. 9.—p. 3
  15. I.V. Kityk, R.I. Mervinskii, J. Kasprczyk, S. Jossi, Synthesis and properties of nm-sized single crystals embedded in photopolymeric host. *Mater. Lett.* **27**, 233–237 (1996)
  16. S. Tkaczyk, M. Galceran, S. Kret, M.C. Pujol, M. Aguiló, F. Diaz, A.H. Reshak, I.V. Kityk, UV-excited piezooptical effects in oxide nanocrystals incorporated into PMMA matrices. *Acta Mater.* **56**, 5677–5684 (2008)
  17. M.K. Balakirev, V.A. Smirnov, L.I. Vostrikova, I.V. Kityk, J. Kasprczyk, W. Gruhn, Giant increase of the second harmonic radiation's absorption during optical poling of oxide glass. *J. Mod. Opt.* **50**, 1237–1244 (2003)
  18. I.V. Kityk, J. Kasprczyk, B. Sahraoui, M.F. Yasinskii, B. Holan, Low temperature anomalies in polyvinyl alcohol photopolymers. *Polymers* **38**, 4803–4806 (1997)
  19. I.V. Kityk, A. Majchrowski, B. Sahraoui, IR-induced nonlinear optics in Ge-doped Bi<sub>12</sub>TiO<sub>20</sub> large-sized nanocrystallites. *Opt. Lasers Eng.* **43**, 75–83 (2005)
  20. K. Ozga, UV-laser induced birefringence in oligoetheracrylate photopolymers. *Opt. Laser Technol.* **98**, 404–408 (2018)
  21. I. Fuks-Janczarek, I.V. Kityk, R. Miedzinski, E. Gondek, J. Ebothe, I. Nzoghe-Mendome, A. Danel, Push-pull benzoxazole based stilbenes as new promising electrooptics materials. *J. Mater. Sci.: Mater. Electron.* **18**, 519–526 (2007)

**Publisher's Note** Springer Nature remains neutral with regard to jurisdictional claims in published maps and institutional affiliations.